

A bidirectional tuned liquid column damper for reducing the seismic response of buildings

Luis Rozas^{1,*}, Ruben L. Boroschek², Aldo Tamburrino² and Matías Rojas¹

¹*MSc Earthquake Engineering, University of Chile*

²*Associated Professor, Department of Civil Engineering, University of Chile*

SUMMARY

In this article, a new bidirectional tuned liquid column damper (BTLCD) is proposed for controlling the seismic response of structures. The device acts as two independent and orthogonal tuned liquid column dampers (TLCDs), but due to its configuration, it requires less liquid than two equivalent independent TLCDs. The equations of motion of the system formed by the BTLCD and the primary structure to be controlled are obtained by means of Lagrangian dynamics explicitly considering the non-symmetrical action of the damping forces. First, the primary structure was assumed to have two degrees of freedom (DOFs). Assuming that the system is excited by a base acceleration that can be considered to be a white noise random process, the optimum design parameters of the device were obtained to minimise the response of the primary structure. The optimum design parameters are presented as expressions covering a wide range of possible configurations for the device in a controlled structure. The use of a BTLCD to control the seismic response of several DOF structures was also studied, showing that if the structural response occurs mainly in two perpendicular modes, then the optimum design parameters for two DOF structures can be used. Experimental analyses of the BTLCD are developed in order to verify its dynamical properties. Finally, the device is designed for controlling the seismic response of a six DOF scale model. Numerical analyses are developed in order to verify the effectiveness and accuracy of the equations and design procedures proposed herein. Copyright © 2015 John Wiley & Sons, Ltd.

Received 6 September 2013; Revised 6 June 2015; Accepted 7 August 2015

KEY WORDS: bidirectional; tuned liquid column damper; vibration control; optimal control; passive dampers; random vibrations

1. INTRODUCTION

More than 50% of the world's population lives in cities. The continuous growth of urban areas, together with the development of modern construction techniques, has resulted in an increasing number of tall buildings. These types of structures are characterised by its flexibility, with long vibration periods and low intrinsic damping. Consequently, when subjected to dynamic loads such as earthquakes, tall buildings develop oscillations that may persist long after the events themselves have ceased. The vibration levels of such structures may exceed the serviceability criteria, causing discomfort to occupants. In some cases, the vibration may even be greater than the agreed safe levels, causing possible damage to nonstructural or structural components. Several devices have been proposed to reduce the structural response of tall buildings. Among these, passive energy dissipation devices have been widely accepted and used in several structures [1]. These types of devices absorb part of the energy supplied to the structure by external actions, such as winds or earthquakes, thereby reducing its response. As shown by Feng and Mita, taking advantage of the structural subconfiguration usually found in tall buildings, part of the structure itself can also be used to absorb this external energy without adding extra mass [2]. Following a similar strategy, Maurizio De Angelis *et al.* [3] investigated the dynamic response of a building with large mass ratio tuned

*Correspondence to: Luis T. Rozas, MSc Earthquake Engineering, University of Chile, Chile.

†E-mail: lrozas@ing.uchile.cl

mass dampers (TMD), in which part of the structure itself is used as tuned mass. In this line of work, Roberto Villaverde *et al.* [4] proposed the detachment of a building's roof through the insertion of sliding bearings and steel oval-shaped elements, to form a simple resonant oscillator, which counteracts the building oscillation. Numerous investigations regarding the determination of the optimum tuning parameters of TMD have been developed, among which may be mentioned the work of Tsai and Lin [5], who proposed optimum tuning parameters for support-excited structures subject to harmonic excitations, Sadek F. *et al.* [6] who derived the optimal tuning parameters in order to provide large damping ratios for the first two vibration modes of the controlled structure. A detailed study of the optimal design methods for combined passive viscous dampers with TMD's can be found in the work of Takewaki [7]. Although there are many kinds of passive dampers, tuned liquid dampers (TLD) stand out due to its advantages, such as their low cost of manufacture and maintenance. There is also practically no weight penalty to the building if the water is used for other purposes such as to prevent the spread of fire, or for drinking.

One key type of TLD is the tuned liquid column damper (TLCD). First proposed by Sakai *et al.* [8], in essence, this device consists of a U-shaped liquid tank. When the device is subject to an external perturbation causing a displacement of the free surface of the liquid, gravity acts as a restoring force, allowing it to oscillate. A restriction is positioned in the centre of the horizontal section of the device, which together with the friction, and the sudden change in flow direction between the horizontal and vertical sections, produces an energy dissipation mechanism that dampens the oscillation of the liquid. Several investigations have been carried out to determine the optimum design parameters of TLCDs. Gao *et al.* [9] studied TLCD optimisation for sinusoidal type excitations by numerical means. Kareem and Yalla [10] determined the optimum design parameters for one degree of freedom (DOF) primary structures subjected to random-type actions. More recently, Shum *et al.* [11] proposed optimal tuning parameters for base-excited damped structures. Considering the nonclassical nature of the damping forces, Wu and Hsieh studied the dynamic characteristics of the TLCD and showed the existence of two coupled natural frequencies between the primary structure and the device [12]. Wu *et al.* proposed a design guide for TLCDs and primary structures subject to random wind loading [13]. The influence of different fluids and the feasibility of using low viscosity magnetorheological fluids within the TLCD was studied by Colwell and Basu [14] through experimental and theoretical analysis. Ghosh and Basu [15,16] studied an alternative TLCD configuration to control short period and nonlinear structures, connecting the device via a spring to the primary structure to be controlled. Another option for controlling short-period oscillations is the use of pressurized air columns as shown by Shum *et al.* [17]. Others studies on the applications of TLCD include its use on offshore wind turbines subject to the combined action of wind and waves. The study of Colwell and Basu [18] showed that the TLCD can greatly reduce the dynamic response of such structures, but its use can be restricted because of space limitations. The use of multiple TLCDs for seismic applications has also been studied, showing that the use of such configurations does not necessarily imply an improvement in structural control compared with a single TLCD. However, their use increases robustness with respect to errors in estimating the dynamic parameters of the controlled structure [19,20]. Multiple TLCDs have also been studied for the reduction of coupled lateral and torsional vibrations in long span bridges [21,17].

Although the use of TLCDs can be an efficient way of reducing the response of buildings, one major disadvantage is their inability to act in two perpendicular directions. This can be very useful for controlling the structural response of buildings for two perpendicular modes with high participation factors, as in the case of several tall buildings. The vibrational control of such structures using TLCDs has been the subject of research by various investigators. One of the first attempts to use a bidirectional TLCD was made by P. A. Hitchcock in 1997. The device can be regarded as several TLCDs that share a common horizontal mass of water [22]. In 2010, Lee *et al.* proposed the use of a bidirectional tuned and sloshing damper, which acts as a TLCD in one direction and as a sloshing damper in the perpendicular direction [23].

In this paper, a new bidirectional TLCD (BTLCD) is proposed. The device acts like a TLCD in two orthogonal directions; thanks to its configuration, the mass of liquid required is reduced compared with two independent TLCDs. The primary objective of this study was to derive the equations of motion of the system formed by the BTLCD and the primary structure to be controlled, when both are subject to a base acceleration. The formulation of the equations of motion, by means of Lagrangian dynamics,

explicitly considers the non-classical damping inherent in the system. The optimal parameters are derived assuming that the base acceleration can be expressed as a white noise random process. Although several previous investigations have dealt with the determination of the optimal parameters, in this study the non symmetrical action of the damping forces, as shown by Wu and Hsieh [12], are explicitly considered in the derivation of the optimal tuning parameters of the BTLCD. Based on this characterisation, the optimum parameters minimising the mean square displacement of the controlled structure are found for both directions. The optimal design parameters of the device are presented as functions of the mass ratio, μ , the shape factor of the device, ζ , the ratio of the cross-sections of the vertical and horizontal parts of the device, v , and the critical damping ratio for the primary structure, ζ_p . Finally, an optimal design procedure for BTLCD in several degrees of freedom structures is proposed. In this case, the primary structure can be represented, for design purposes, as an equivalent two DOF structure. From this point, the optimal design parameters proposed can be used for the device.

2. BIDIRECTIONAL TUNED LIQUID COLUMN DAMPER DESCRIPTION

The device proposed is shown in Figure 1 and can be regarded as four single TLCDs combined in one unit. The configuration of the BTLCD, which in plan view has the shape of an annular rectangle, can be adjusted to two different frequencies of oscillation by modifying the total length of the liquid conduits. Additionally, the ratio between the cross-section of the horizontal containers, A_x and A_y , and the cross-section of the vertical columns, A_v , can be used to further adjust the natural frequencies of oscillation of the device. A restriction or orifice located in the mid-point of the horizontal tanks is used to control the damping of the oscillation of the liquid inside the device. For the purpose of describing the motion of the liquid mass inside the BTLCD, two DOFs are selected: displacement of the liquid in the containers parallel to the X direction, u_{dx} , and displacement of the liquid in the containers parallel to the Y direction, u_{dy} . The displacement of the free liquid surfaces in the vertical columns can be related to u_{dx} and u_{dy} by considering the fact that the total volume of liquid is always preserved. So, for example, if the displacement of the liquid in both the horizontal conduits is in the direction of one vertical column, then the displacement of the free liquid surface in this vertical column is as follows:

$$u_v = \frac{1}{A_v}(A_y u_{dy} + A_x u_{dx}).$$

The proposed BTLCD also requires less liquid compared with other configurations. In using two single and perpendicular TLCDs, it can be seen that when the oscillation is in one of the principal directions, the liquid in the TLCD oriented perpendicular to this direction performs no useful function, and it becomes a penalty mass. In the BTLCD, it is only the liquid inside the horizontal conduits between the vertical columns that has no use under this condition. The use of TLCDs in a crossed configuration also requires a greater amount of liquid than the proposed BTLCD. This is because of the fact that the BTLCD, understood as four single TLCDs, shares the vertical columns, there being

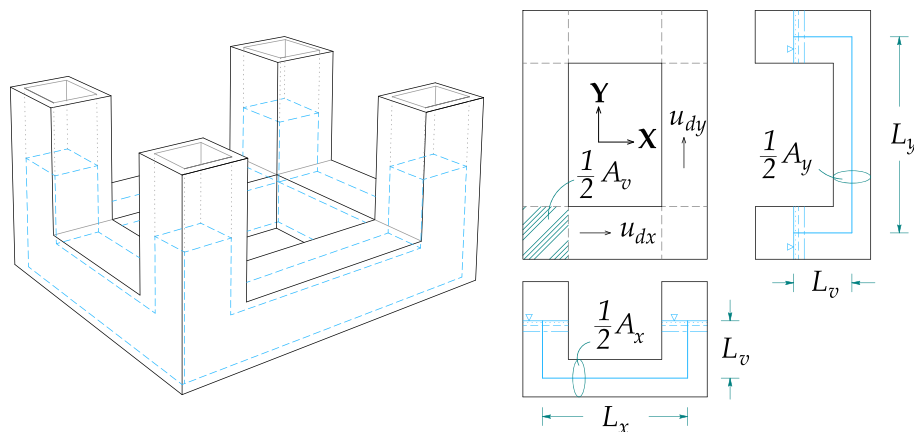


Figure 1. Schematic view of the bidirectional tuned liquid column damper and its main geometrical properties.

no requirement for individual vertical columns for each of the four TLCs. In the alternative of using TLCs combined with sloshing, a relatively large portion of the liquid mass do not participate in the sloshing motion when rectangular tank shapes are used as showed by M. J. Tait [24]. Also in this case, the strong nonlinear behaviour of the sloshing motion, cause that the stiffness and damping depend on the frequency and amplitude of the liquid oscillation [23].

3. BIDIRECTIONAL TUNED LIQUID COLUMN DAMPER AND THE CONTROLLED STRUCTURE EQUATIONS OF MOTION

The system under investigation is shown in Figure 2 and can be separated into two substructures. One of them is the BTLCD and the other is the two-DOF primary structure. As indicated in Section 2, the motion of the liquid inside the BTLCD is defined by u_{dx} and u_{dy} , which measure the displacement of the liquid relative to the mass of the primary structure in the X and Y directions, respectively. The motion of the primary structure is described using the DOF x and y , which measure the relative motion between its mass and the ground in the X and Y directions, respectively. If the entire system is now subject to a base acceleration defined by \ddot{u}_{sx} and \ddot{u}_{sy} , then the equations of motion of the system can be derived using the Lagrange equations [25].

$$\frac{d}{dt} \left(\frac{\partial T}{\partial \dot{q}_i} \right) - \frac{\partial T}{\partial q_i} + \frac{\partial V}{\partial q_i} = Q_i \quad i = 1 \dots n \quad (1)$$

where T and V correspond to the total kinetic energy and the total potential energy of the system, q_i is the i -th generalised coordinate, Q_i is the generalised force associated with q_i , n is the total number of DOF of the system, four in this case, and t is the time.

Assuming that the fluid is incompressible and the transverse velocity profile of the liquid is constant, implying that the fluid flux is turbulent, the kinetic energy and the potential energy for the entire system can be readily obtained. On the other hand, the nonconservative dissipative forces associated with the BTLCD are produced by the flow, which can be divided into three components. The first and most important is caused by the orifice or restriction located at the mid-point of the horizontal conduit. The second is the friction resistance, and the third is a result of the sudden change in direction of the flow at the corners of the device. The nonconservative dissipative forces can be written as follows:

$$Q_{u_{dx}} = -\frac{1}{2} \rho_f \eta_x A_x |\dot{u}_{dx}| \dot{u}_{dx} = -c_{dx} \dot{u}_{dx}; \quad Q_{u_{dy}} = -\frac{1}{2} \rho_f \eta_y A_y |\dot{u}_{dy}| \dot{u}_{dy} = -c_{dy} \dot{u}_{dy} \quad (2)$$

where η_x and η_y are the flow resistance coefficients in the X and Y direction, respectively. As seen from Equation 2, the forces $Q_{u_{dx}}$ and $Q_{u_{dy}}$ are nonlinear. For design purposes, we need to express these forces

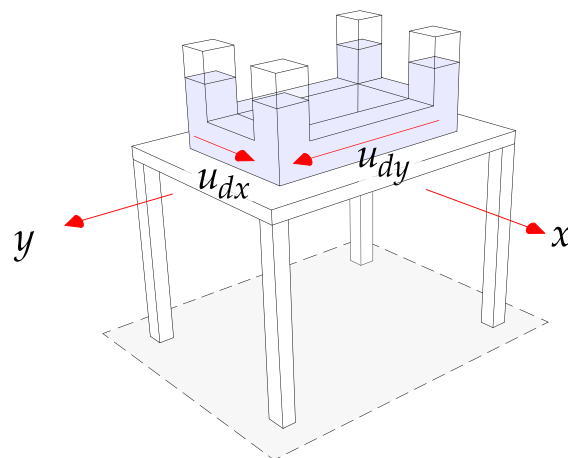


Figure 2. A two degrees of freedom primary structure with a bidirectional tuned liquid column damper.

as linear equivalents by means of the coefficients c_{dx} and c_{dy} [13]. Using stochastic equivalent linearization, these nonlinear damping terms can be replaced by equivalent linear ones, as shown in the following section. The nonconservative dissipative forces associated with the primary structure can be written as follows:

$$Q_x = \frac{1}{2} \rho_f \eta A_x |\dot{u}_{dx}| \dot{u}_{dx} - C_x \dot{x} = c_{dx} \dot{u}_{dx} - C_x \dot{x}; \quad Q_y = \frac{1}{2} \rho_f \eta A_y |\dot{u}_{dy}| \dot{u}_{dy} - C_y \dot{y} = c_{dy} \dot{u}_{dy} - C_y \dot{y} \quad (3)$$

The equations of motion of the system can now be obtained by substituting the corresponding terms into the Lagrangian equations. By doing, so we obtain the following:

$$\left. \begin{aligned} M_T \ddot{x} + C_x \dot{x} + K_x x &= -M_T \ddot{u}_{sx} + c_{dx} \dot{u}_{dx} - m_{hx} \ddot{u}_{dx} \\ M_T \ddot{y} + C_y \dot{y} + K_y y &= -M_T \ddot{u}_{sy} + c_{dy} \dot{u}_{dy} - m_{hy} \ddot{u}_{dy} \\ m_{ex} \ddot{u}_{dx} + v_x c_{dx} \dot{u}_{dx} + k_{dx} u_{dx} &= -m_{hx} v_x (\ddot{u}_{sx} + \ddot{x}) \\ m_{ey} \ddot{u}_{dy} + v_y c_{dy} \dot{u}_{dy} + k_{dy} u_{dy} &= -m_{hy} v_y (\ddot{u}_{sy} + \ddot{y}) \end{aligned} \right\} \quad (4)$$

where $M_T = m_p + m_f + m_u$ is the total mass of the system; $m_{hx} = A_x L_x \rho_f$ and $m_{hy} = A_y L_y \rho_f$ are the liquid mass inside the horizontal conduits parallel to the X and Y directions, respectively; $v_x = A_v/A_x$ and $v_y = A_v/A_y$ are the quotients between the areas of the vertical columns and the horizontal conduits in the X and Y directions, respectively; m_{ex} and m_{ey} are the effective liquid masses in the X and Y directions, and are defined by $m_{ex} = A_x L_{ex} \rho_f$ and $m_{ey} = A_y L_{ey} \rho_f$, where $L_{ex} = v_x L_x + 2L_v$ and $L_{ey} = v_y L_y + 2L_v$ are the effective lengths in the X and Y directions; and finally, $k_{dx} = 2A_x \rho_f g$ and $k_{dy} = 2A_y \rho_f g$ are the equivalent stiffness of the device.

In order to obtain more general results from the equations of motion, the system 4 can be rewritten using nondimensional parameters, resulting in the following system of equations:

$$\left. \begin{aligned} \alpha_x \ddot{x} + 2\alpha_x \omega_{px} \zeta_{px} \dot{x} + \alpha_x \omega_{px}^2 x &= -\alpha_x \ddot{u}_{sx} + 2\omega_{dx} \zeta_{dx} \mu_x \dot{u}_{dx} - \alpha_x^2 \ddot{u}_{dx} \\ \alpha_y \ddot{y} + 2\alpha_y \omega_{py} \zeta_{py} \dot{y} + \alpha_y \omega_{py}^2 y &= -\alpha_y \ddot{u}_{sy} + 2\omega_{dy} \zeta_{dy} \mu_y \dot{u}_{dy} - \alpha_y^2 \ddot{u}_{dy} \\ \ddot{u}_{dx} + 2v_x \omega_{dx} \zeta_{dx} \dot{u}_{dx} + \omega_{dx}^2 u_{dx} &= -\alpha_x v_x (\ddot{u}_{sx} + \ddot{x}) \\ \ddot{u}_{dy} + 2v_y \omega_{dy} \zeta_{dy} \dot{u}_{dy} + \omega_{dy}^2 u_{dy} &= -\alpha_y v_y (\ddot{u}_{sy} + \ddot{y}) \end{aligned} \right\} \quad (5)$$

In the system of Equations 5, the parameters $\omega_{dx} = \sqrt{2g/L_{ex}}$ and $\omega_{dy} = \sqrt{2g/L_{ey}}$ are the natural frequencies of oscillation of the device; $\omega_{px} = \sqrt{K_x/M_T}$ and $\omega_{py} = \sqrt{K_y/M_T}$ are the frequencies of oscillation of a structure with the same stiffness as the primary structure, but with a mass equal to the total mass of the system; $\zeta_{dx} = c_{dx}/2m_{ex}\omega_{dx}$ and $\zeta_{dy} = c_{dy}/2m_{ey}\omega_{dy}$ are the critical damping ratios of the device; $\zeta_{px} = C_x/2M_T\omega_{px}$ and $\zeta_{py} = C_y/2M_T\omega_{py}$ are the critical damping ratios of the structure with the same stiffness as the primary structure, but with a mass equal to the total mass of the system. The parameters $\alpha_x = L_x/L_{ex}$ and $\alpha_y = L_y/L_{ey}$ can be related to the terms $\zeta_x = L_x/(L_x + 2L_v)$ and $\zeta_y = L_y/(L_y + 2L_v)$, which essentially define the shape factors of the device. It is clear that when $v_x = v_y = 1$, then $\alpha_x = \zeta_x$ and $\alpha_y = \zeta_y$. In general, the following relationship can be found between the α and ζ terms:

$$\alpha = \frac{\zeta}{\zeta(v - 1) + 1} \quad (6)$$

in which subscripts have been removed for clarity. Because of the fact that ζ is always less than one, it is easy to show, using the relation 6, that the inequality $\alpha \cdot v < 1$ will be retained. The parameters $\mu_x = m_{hx}/M_T$ and $\mu_y = m_{hy}/M_T$ are the mass ratios between the liquid mass inside the horizontal conduits and the total mass of the system. These parameters can be expressed in terms of the quotients between the total liquid mass in the X and Y directions and the total mass of the system, $\mu_{fx} = \rho_f A_x (L_x + 2L_v)/M_T$ and $\mu_{fy} = \rho_f A_y (L_y + 2L_v)/M_T$, as follows:

$$\mu = \left(\frac{\alpha}{\alpha(1 - v^2) + v} \right) \mu_f \quad (7)$$

3.1. Equivalent damping for random base acceleration

The nonlinear equations of motion derived in the previous section can be replaced by equivalent linear ones with known solutions. The difference, or error, between the linear equivalent representation and the actual nonlinear one can be written as $\varepsilon = c_d \dot{u}_d - C_{NL}(u_d, \dot{u}_d) \dot{u}_d$ (directional subscripts will be

omitted for clarity), where $C_{NL}(u_d, \dot{u}_d)$ represent in general terms the nonlinear damping force. In this case, the expression of $C_{NL}(u_d, \dot{u}_d)$ is a function of the flow resistance. Assuming the flow is turbulent [26,27], and minimising the mean square value of the error, $\mathbb{E}\{e^2\}$, it can be shown that [28,29]

$$c_d = \sqrt{\frac{2}{\pi}} \rho_f A v^2 \eta \sigma \dot{u}_d \quad (8)$$

Where it is assumed that the probability density function of the nonlinear damping force is Gaussian [28,13,29]. Equation 8 can be rewritten as

$$\eta = \sqrt{2\pi} \frac{m_e \omega_d \zeta_d}{A v^2 \rho_f \sigma \dot{u}_d} \quad (9)$$

From Equation 9, the flow resistance coefficient can be obtained as a function of the frequency of oscillation, ω_d , and the critical damping ratio of the device, ζ_d .

4. BIDIRECTIONAL TUNED LIQUID COLUMN DAMPER OPTIMUM DESIGN PARAMETERS FOR RANDOM WHITE NOISE BASE ACCELERATION

4.1. Undamped primary structure

As previously shown, the equations of motion are uncoupled for the X and Y directions. For this reason, the following analysis applies for both directions. Assuming that the base acceleration is represented by a Gaussian white noise process with constant power spectral density \ddot{u}_{so} , the mean square displacement response of the primary structure can be expressed as [30]:

$$\mathbb{E}\{x^2\} = \ddot{u}_{so} \int_{-\infty}^{\infty} |H_x(\omega)|^2 d\omega \quad (10)$$

where $H_x(\omega)$ is the transfer function between the base acceleration and the displacement of the primary structure in the X direction. This function can be expressed in terms of the nondimensional frequency $\rho = \Omega/\omega_p$, (where Ω is the frequency of the external excitation), as follows [30,31]:

$$H_x(\rho) = \frac{1}{\omega_p^2} \cdot \frac{B_2 \rho^2 + i B_1 \rho + B_0}{A_4 \rho^4 + i A_3 \rho^3 + A_2 \rho^2 + i A_1 \rho + A_0} \quad (11)$$

The terms A and B are detailed as follows:

$$\begin{aligned} A_0 &= f^2 & A_4 &= 1 - \mu \alpha v \\ A_1 &= 2f(f\zeta_p + v\zeta_d) & B_0 &= -f^2 \\ A_2 &= -(1 + f^2 + 4\zeta_p \zeta_d f) & B_1 &= -2f\zeta_d v(1 + \mu) \\ A_3 &= -2(\zeta_p + \zeta_d f v(1 + \mu)) & B_2 &= 1 - \mu \alpha v \end{aligned} \quad (12)$$

where $f = \omega_d/\omega_p$ is the frequency ratio. The integral in Equation 10 can be evaluated using integral tables [30], resulting in

$$\mathbb{E}\{x^2\} = \frac{\pi \ddot{u}_{so}}{\omega_p^3} \cdot \frac{\left(\frac{B_0^2}{A_0}\right) (A_2 A_3 - A_1 A_4) - A_3 (B_1^2 + 2B_0 B_2) + A_1 B_2^2}{A_1 (A_2 A_3 - A_1 A_4) - A_0 A_3^2} \quad (13)$$

As shown in Section 6, in order to complete the design of the BTLCD, it is also necessary to find the mean square of the displacement of the liquid in the device, $\mathbb{E}\{u_d^2\}$, and the mean square value of its velocity, $\mathbb{E}\{\dot{u}_d^2\}$. These parameters can be obtained from Equations 14 and 15 as follows [30,31]:

$$\mathbb{E}\{u_d^2\} = \frac{\omega_p}{\omega_d^4} \int_{-\infty}^{\infty} \left| \frac{iC_1\rho + C_0}{A_4\rho^4 + iA_3\rho^3 + A_2\rho^2 + iA_1\rho + A_0} \right|^2 S(\rho) d\rho \tag{14}$$

$$\mathbb{E}\{\dot{u}_d^2\} = \frac{\omega_p}{\omega_d^2} \int_{-\infty}^{\infty} \left| \frac{D_1\rho^2 + iD_0\rho}{A_4\rho^4 + iA_3\rho^3 + A_2\rho^2 + iA_1\rho + A_0} \right|^2 S(\rho) d\rho \tag{15}$$

where $S(\rho)$ is the mean square of the spectral density in terms of the nondimensional parameter ρ . If the process is assumed to be a white noise random process with constant power spectral density, \ddot{u}_{so} , the foregoing expressions can then be reduced to the following:

$$\mathbb{E}\{u_d^2\} = \frac{\pi\ddot{u}_{so}\omega_p}{\omega_d^4} \cdot \frac{\left(\frac{C_0}{A_0}\right)(A_2A_3 - A_1A_4) - A_3C_1^2}{A_1(A_2A_3 - A_1A_4) - A_0A_3^2} \tag{16}$$

$$\mathbb{E}\{\dot{u}_d^2\} = \frac{\pi\ddot{u}_{so}\omega_p}{\omega_d^2} \cdot \frac{A_1D_1^2 - A_3D_0^2}{A_1(A_2A_3 - A_1A_4) - A_0A_3^2} \tag{17}$$

where the expressions for the terms C and D are as follows:

$$\begin{aligned} C_0 &= -\alpha f^2 & D_0 &= -\alpha f \\ C_1 &= -2\alpha\zeta_p v f^2 & D_1 &= 2\alpha\zeta_p v f \end{aligned} \tag{18}$$

Returning to Equation 13, the mean square of the displacement of the primary structure can be obtained as a function of $\mu, \zeta_p, \alpha, v, \zeta_d$ and f . The value of ζ_p is mainly given by the problem itself and can be related to μ and α . The parameters μ, α and v can be determined by the designer at an early stage. It can also be shown that the optimal value of v is 1 [13], and as the value of ζ ($\zeta = \alpha$ when $v = 1$) approaches to 1, the reduction in the response of the primary structure increases [13,31]. This implies that a device with equal cross-sections ($A_v = A_x = A_y$) and with the largest possible horizontal dimension is always preferable. Of course, it is not always possible to obtain these conditions, but they nevertheless represent a desirable design. For instance, architectonic restrictions may not allow large plan dimensions of the device, forcing the reduction of the shape factor ζ . This leaves two remaining parameters: f and ζ_d . The optimal values of these parameters are obtained by minimising $\mathbb{E}\{x^2\}$ given by Equation 13. If the damping of the primary structure can be neglected, then closed expressions for the optimum design parameters can be derived. These expressions are shown in Equations 19 and 20 and graphically in Figure 3:

$$f|_{OPT} = \sqrt{\frac{2\mu\alpha v[\mu(1 - \alpha v(2 + \mu)) + 1 - \frac{3}{2}\alpha v] + 2\alpha v - \mu}{(1 + \mu)[2\mu\alpha v(\mu + \frac{3}{2}) + 2\alpha v - \mu]}} \tag{19}$$

$$\zeta_d|_{OPT} = \frac{\alpha}{2} \sqrt{\frac{\mu[4\mu^2\alpha v(\alpha v(\mu + 2) - 1) + 6\mu\alpha v(\frac{3}{2}\alpha v - 1) + \mu - 4\alpha v]}{[2\mu\alpha v(\mu + \frac{3}{2}) + 2\alpha v - \mu][2\mu^2\alpha v(\alpha v(\mu + 2) - 1) + 2\mu\alpha v(\frac{3}{2}\alpha v - 1) - 2\alpha v + \mu]}} \tag{20}$$

Figure 3 indicates that the higher the mass ratio, the lower the optimum frequency ratio f and the higher the optimum critical damping ratio of the device, ζ_d . Another important conclusion from Figure 3 is that when $\mu \rightarrow 0$, then the optimum frequency ratio equals 1, meaning that the natural frequency of oscillation of the device will equal the natural frequency of oscillation of the primary structure, which is also consistent with its expected behaviour.

4.2. Damped primary structure

Unlike the previous case, obtaining closed expressions for the optimum design parameters f and ζ_d is far too complex, and a numerical optimisation procedure must be used instead. Here, we use the

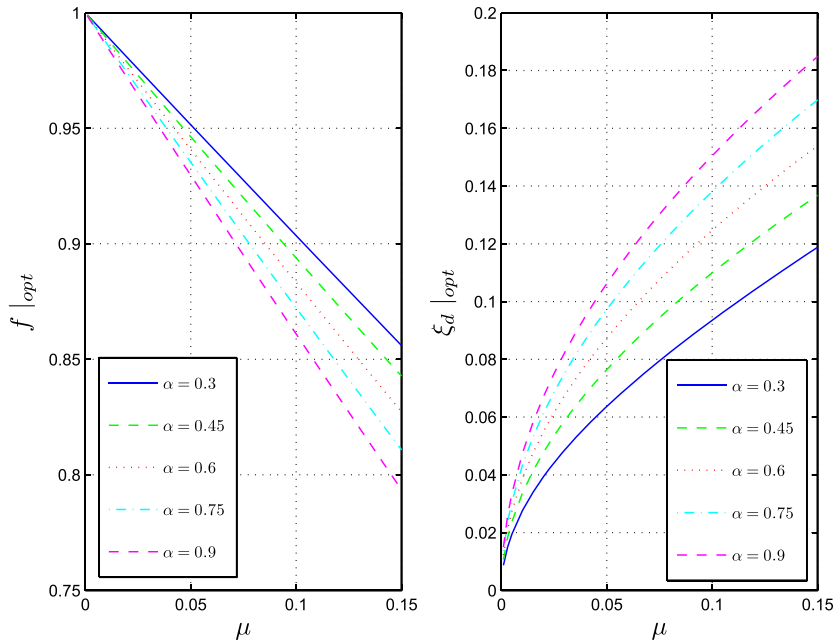


Figure 3. Bidirectional tuned liquid column damper optimum design parameters for random white noise acceleration, an undamped primary structure and $v = 1$.

normalised mean square of the displacement of the primary structure as the parameter to be minimised, which is defined as follows:

$$\overline{\mathbb{E}\{x^2\}} = \frac{\mathbb{E}\{x^2\}}{\mathbb{E}^*\{x^2\}} \tag{21}$$

where $\mathbb{E}^*\{x^2\}$ is the mean square of the displacement of the structure, with the same stiffness and damping as the structure to be controlled, but with a mass equal to the total mass of the system, that is, [30]: $\mathbb{E}^*\{x^2\} = \pi \ddot{u}_{so} / 2 \zeta_p \omega_p^3$.

In Figure 4, $\overline{\mathbb{E}\{x^2\}}$ is plotted against f and ζ_d for two different initial design conditions. It is easy to note that a minimum exists for a particular combination of values of f and ζ_d , these being the optimum

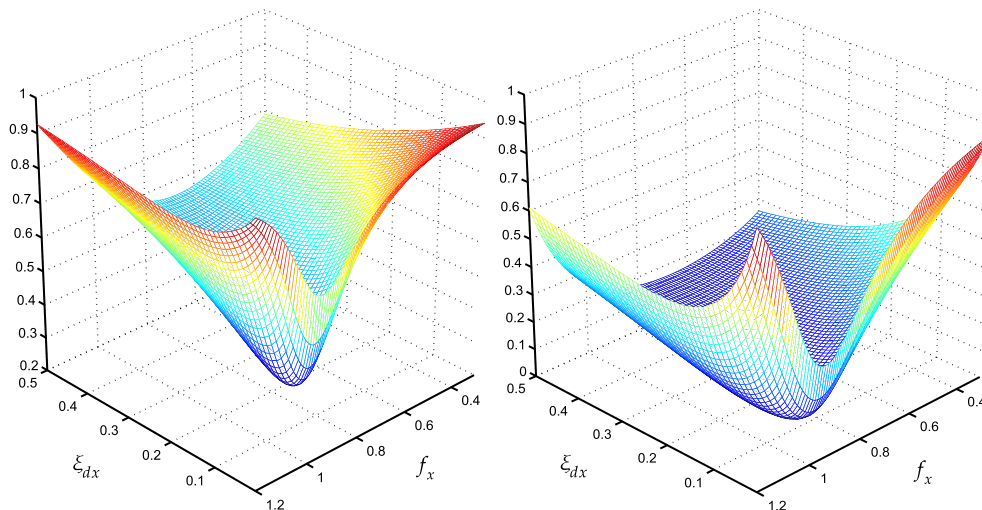


Figure 4. Normalised mean square value $\overline{\mathbb{E}\{x^2\}}$, as a function of f and ζ_d . The left graph is for $\mu = 0.03$ and $\zeta_p = 0.02$, and the right graph is for $\mu = 0.05$ and $\zeta_p = 0.005$. In both cases, $v = 1$ and $\alpha = 0.75$.

design parameters to be found. In order to provide design expressions that cover most practical cases, the numerical optimisation was performed considering the following range of values: $0.001 \leq \mu \leq 0.15$; $0.4 \leq \alpha \leq 0.95$; $0.005 \leq \xi_p \leq 0.1$ and $\nu = 1$.

In Figure 5, the results of the numerical optimisation procedure are shown. It can be seen that the value of the optimum frequency ratio decreases when the mass ratio increases; in contrast, the optimum device critical damping ratio increases. Also, both the optimal frequency ratio and the optimal damping ratio decreases as the critical damping ratio of the primary structure increases. A closer look at the values of optimum frequency ratio when $\mu \rightarrow 0$ and $\nu = 1$ leads to the conclusion that these are equal to $\sqrt{1 - 2\xi_p^2}$. This conclusion can be interpreted physically if we consider the fact that the device controls the response via resonance. Remembering that the displacement resonance frequency of the structure without the device is equal to $\omega_n \sqrt{1 - 2\xi_p^2}$, it remains clear that when $\mu \rightarrow 0$, the optimal frequency ratio is $\sqrt{1 - 2\xi_p^2}$. Using this result, we can calibrate a numerical expression for the optimum frequency ratio, $f|_{OPT}$, as function of μ , α , and ξ_p for $\nu = 1$ as follows:

$$f|_{OPT} = f|_{OPT}(\xi_p = 0) + \sqrt{1 - 2\xi_p^2} - 1 + \Delta f \tag{22}$$

where the first term of the right-hand side of Equation 22 is the optimum frequency ratio for the undamped primary structure, Equation 19, the second term is the optimal frequency ratio when $\mu \rightarrow 0$, and Δf is the difference between these terms and the optimal frequency ratio obtained by the numerical optimisation procedure. Using curve fitting, Δf can be adjusted as a power function of μ , as shown in Equation 23. This equation used in combination with Equation 22 gives a close approximation to the optimal frequency ratio found by numerical optimisation procedure.

$$\Delta f = (1.2\alpha + 1.285)\xi_p\mu^{[(2.346 - 0.793\alpha)\xi_p^2 + (0.67\alpha - 1.492)\xi_p + 0.466]} \tag{23}$$

The values of the optimum critical damping ratio of the device can also be adjusted using curve fitting. In this case, the optimal damping ratio can be written as follows:

$$\xi_d|_{OPT} = \xi_d|_{OPT}(\xi_p = 0) - \Delta \xi_d \tag{24}$$

where $\Delta \xi_d$ is the difference between the optimum damping values for undamped primary structure, Equation 19, and those obtained by the numerical optimisation procedure for the damped

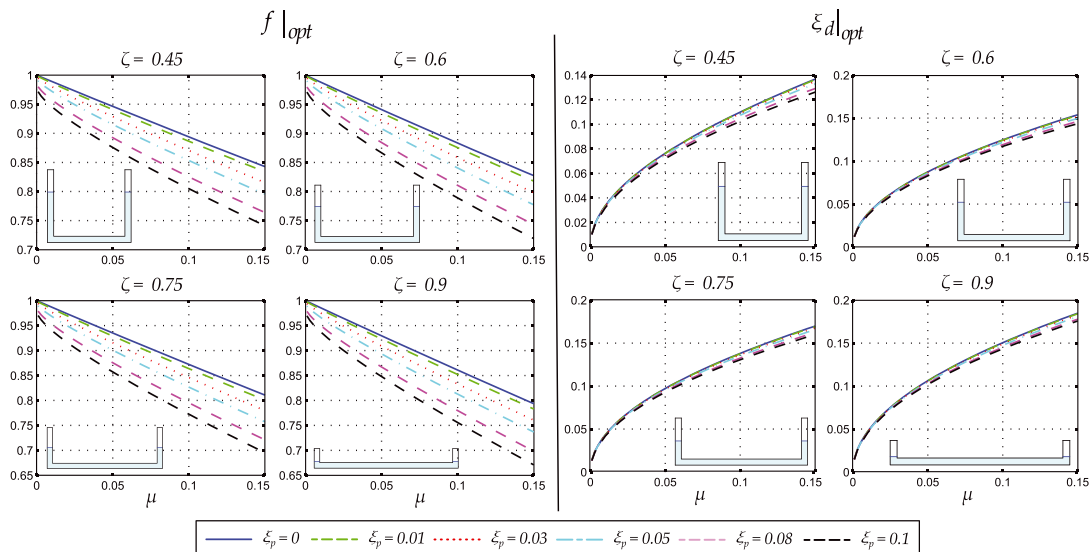


Figure 5. Optimum frequency ratios, left, and optimum critical damping ratios, right, for $\nu = 1$.

primary structure. The difference, $\Delta \xi_d$, is again adjusted as a power function in μ , for $v=1$, as follows:

$$\Delta \xi_d = (0.557 - 0.235\alpha)\xi_p\mu^{[(8.955\alpha-31.243)\xi_p^2+(1.738-0.782\alpha)\xi_p+0.953-0.169\alpha]} \tag{25}$$

Equation 25 used in combination with expression 20 returns the optimal critical damping ratio of the device for the damped primary structure. Again, the results obtained using these equations are in good agreement with the numerical optimisation results.

5. BIDIRECTIONAL TUNED LIQUID COLUMN DAMPER FOR SEVERAL DEGREES OF FREEDOM STRUCTURES

Consider the several degrees of freedom structure with BTLCD shown in Figure 6. The equations of motion can be found by means of the Lagrange equations for the system, which can be written in vector notation as [25] follows:

$$\frac{d}{dt} \left\{ \frac{\partial T}{\partial \dot{U}} \right\} - \left\{ \frac{\partial T}{\partial U} \right\} + \left\{ \frac{\partial V}{\partial U} \right\} = \{Q\} \tag{26}$$

In this case, we have a total of $2N+2$ equations of motion, N being the total number of levels of the primary structure. The nonconservative dissipative forces associated with the primary structure can be expressed as follows:

$$Q_j = -\{\delta_{kj}\}^T [C_p] \{\dot{U}_p\} + [L] \begin{bmatrix} c_{dx} & 0 \\ 0 & c_{dy} \end{bmatrix} [L]^T \begin{Bmatrix} \dot{u}_{dx} \\ \dot{u}_{dy} \end{Bmatrix} \quad j = 1 \dots 2N \tag{27}$$

where the first term in the right-hand side of Equation 27 are the dissipative forces due to the inherent damping of the structure and $\{\delta_{kj}\}$ is Kronecker delta vector. The second term represents the dissipative forces transmitted from the BTLCD to the primary structure, being $[L]$ the matrix that defines the location of the BTLCD. If the BTLCD is located in the i -th level of the structure then

$$[L]^T = \begin{bmatrix} 0 & \dots & 1 & \dots & 0 & 0 & \dots & 0 \\ 0 & \dots & 0 & 0 & \dots & 1 & \dots & 0 \\ 1 & & i & & & & i+N & 2N \end{bmatrix} \tag{28}$$

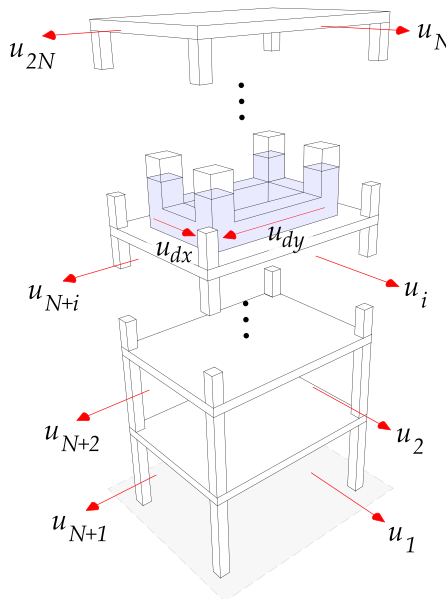


Figure 6. Several degrees of freedom structure with a bidirectional tuned liquid column damper.

On the other side, the nonconservative forces associated with the BTLCD are $Q_{2N+1} = -c_{dx}\dot{u}_{dx}$ and $Q_{2N+2} = -c_{dy}\dot{u}_{dy}$. Once the kinetic energy and potential energy are found, the equations of motion of the entire system can be written as follows:

$$\begin{bmatrix} [\overline{M}_p] & [M_{pd}] \\ [M_{pd}]^T & \begin{bmatrix} m_{ex}/v_x & 0 \\ 0 & m_{ey}/v_y \end{bmatrix} \end{bmatrix} \begin{Bmatrix} \{\dot{U}_p\} \\ \ddot{u}_{dx} \\ \ddot{u}_{dy} \end{Bmatrix} + \begin{bmatrix} [C_p] & [C_{pd}] \\ [0] & \begin{bmatrix} c_{dx} & 0 \\ 0 & c_{dy} \end{bmatrix} \end{bmatrix} \begin{Bmatrix} \{\dot{U}_p\} \\ \dot{u}_{dx} \\ \dot{u}_{dy} \end{Bmatrix} + \begin{bmatrix} [K_p] & [0] \\ [0] & \begin{bmatrix} k_{dx}/v_x & 0 \\ 0 & k_{dy}/v_y \end{bmatrix} \end{bmatrix} \begin{Bmatrix} \{U_p\} \\ u_{dx} \\ u_{dy} \end{Bmatrix} = - \begin{bmatrix} [\overline{M}_p] & [M_{pd}] \\ [M_{pd}]^T & \begin{bmatrix} m_{ex} & 0 \\ 0 & m_{ey} \end{bmatrix} \end{bmatrix} \begin{Bmatrix} [r] \\ [0] \end{Bmatrix} \{\ddot{u}_s\} \tag{29}$$

where

$$\begin{aligned} [\overline{M}_p] &= [M_p] + [L] \begin{bmatrix} m_f + m_u & 0 \\ 0 & m_f + m_u \end{bmatrix} [L]^T; [M_{pd}] = [L] \begin{bmatrix} m_{hx} & 0 \\ 0 & m_{hy} \end{bmatrix}; [C_{pd}] \\ &= [L] \begin{bmatrix} c_{dx} & 0 \\ 0 & c_{dy} \end{bmatrix} \end{aligned} \tag{30}$$

where $\{U_p\}$ are the degrees of freedom of the primary structure, $[r]$ is the influence matrix of $\{U_p\}$, and $\{u_s\} = \langle u_{sx}, u_{sy} \rangle^T$ is the vector of the external displacements. It should be noted that the $(1, i)$ and $(2, N + i)$ components of the influence matrix should be equal to 1 and $[M_p]$, $[C_p]$ and $[K_p]$ are the mass damping and stiffness matrix of the primary structure.

Examining the system of Equation 29, it remains clear that the damping matrix is non-symmetrical. The last two equations of the system 37, which describe the motion of the liquid inside the device, remain as follows:

$$\left. \begin{aligned} m_{ex}\ddot{u}_{dx} + v_x c_{dx}\dot{u}_{dx} + k_{dx}u_{dx} &= -m_{hx}v_x(\ddot{u}_{sx} + \ddot{u}_i) \\ m_{ey}\ddot{u}_{dy} + v_y c_{dy}\dot{u}_{dy} + k_{dy}u_{dy} &= -m_{hy}v_y(\ddot{u}_{sy} + \ddot{u}_{i+N}) \end{aligned} \right\} \tag{31}$$

The first $2N$ equations of the system 29 can be rewritten in terms of modal coordinates, $\{U_p\} = [\Phi] \{q\}$, after premultiplying these equations by $[\Phi]^T$. Assuming classic damping matrix of the primary structure, we can write the j -th Equation of 29 as follows:

$$\begin{aligned} \mathbf{m}_j \ddot{q}_j + \mathbf{c}_j \dot{q}_j + \mathbf{k}_j q_j &= - \sum_{k=1}^{2N} \phi_{k,j} M_k \ddot{u}_s - \phi_{i,j} [(m_f + m_u)(\ddot{u}_i + \ddot{u}_s) - c_{dx}\dot{u}_{dx} + m_{hx}\ddot{u}_{dx}] - \\ &\phi_{i+N,j} [(m_f + m_u)(\ddot{u}_{i+N} + \ddot{u}_s) - c_{dy}\dot{u}_{dy} + m_{hy}\ddot{u}_{dy}] \end{aligned} \tag{32}$$

If we need to control vibrational modes along two orthogonal directions simultaneously, and these modes are widely representative of the structural response, we can express the displacements of the i -th level of the primary structure as $u_i \approx \phi_{i,r} q_r$; $u_{i+N} \approx \phi_{i+N,s} q_s$, where r and s are the controlled modes in two perpendicular directions. Using the foregoing approximations, Equation 32 can be reduced to the following two equations of motion for the coordinates u_i and u_{i+N} :

$$\left. \begin{aligned} (\tilde{m}_r + m_f + m_u)\ddot{u}_i + \tilde{c}_r \dot{u}_i + \tilde{k}_r u_i &= -(\Gamma_r \tilde{m}_r + m_f + m_u)\ddot{u}_s + c_{dx}\dot{u}_{dx} - m_{hx}\ddot{u}_{dx} \\ (\tilde{m}_s + m_f + m_u)\ddot{u}_{i+N} + \tilde{c}_s \dot{u}_{i+N} + \tilde{k}_s u_{i+N} &= -(\Gamma_s \tilde{m}_s + m_f + m_u)\ddot{u}_s + c_{dy}\dot{u}_{dy} - m_{hy}\ddot{u}_{dy} \end{aligned} \right\} \tag{33}$$

where $\tilde{m}_r = m_r / \phi_{i,r}^2$, $\tilde{c}_r = c_r / \phi_{i,r}^2$ and $\tilde{k}_r = k_r / \phi_{i,r}^2$, being \tilde{m}_r the equivalent mass of the several DOF primary structure for the r -th mode, \tilde{k}_r the equivalent stiffness of the several DOF primary structure for the r -th mode, and \tilde{c}_r the equivalent damping of the several DOF primary structure for the r -th mode. The definitions of terms \tilde{m}_s , \tilde{c}_s and \tilde{k}_s are analogous but in this case use $i + N$ instead of i . A closer look at the latter definitions shows that the optimal location of the device should be at the position with the largest modal component. This reduces the mass of the equivalent structure, \tilde{m}_r , to its minimum possible value, thereby yielding the largest possible mass ratio between the device and the equivalent

structure. If we examine the system of Equations 33 and 31, and compare them with the system 4, it remains clear that they differ only in the terms Γ_r and Γ_s . Thus, for design purposes, the Several DOF structure can be reduced to an equivalent two DOF. From this point, the optimal design parameters proposed in this investigation can be used to design the BTLCD.

6. BIDIRECTIONAL TUNED LIQUID COLUMN DAMPER DESIGN PROCEDURE

The first step in the design procedure is the estimation of the appropriate mass ratios and shape factors of the device. In practice, a number of factors may constrain the selection of these parameters. For instance, restrictions to the maximum allowable weight that can be added to the structure will limit the mass ratio and, as previously mentioned, space and architectonic limitations may force the use of low values for shape factors. Once the mass ratios, μ_x and μ_y , and one of the shape factors of the device, say the shape factor in the X direction, ζ_x , have been defined, the liquid mass in the X direction can then be calculated as follows:

$$m_{fx} = \frac{\mu_x \mu_y (M_{y_{eq}} - M_{x_{eq}}) + \mu_x (M_{x_{eq}} + m_u)}{\zeta_x (1 - \mu_y) - \mu_x} \quad (34)$$

In Equation 34, it is assumed that the area ratio in the X direction is equal to 1 ($v_x = 1$), which is also its optimum value [13], and that $M_{x_{eq}} = \tilde{m}_r$ and $M_{y_{eq}} = \tilde{m}_s$, where r and s are the modes to be controlled by the device in the X and Y direction, respectively. The total liquid mass in the Y direction can be expressed as follows:

$$m_{fy} = \frac{1}{1 - \mu_y} \left[m_{fx} (\zeta_x (\mu_y - 1) + 1) + \mu_y (M_{y_{eq}} + m_u) \right] \quad (35)$$

The total liquid mass inside the device can be estimated for design purposes as follows: $m_f = m_{fy} + \zeta_x m_{fx}$. The optimum frequency ratio in the X direction, $f_x|_{OPT}$, can be calculated from Equation 19 in the case of negligible damping of the primary structure, or using Equation 22 otherwise. From this value, the optimal frequency of oscillation is determined as follows: $\omega_{dx} = f_x|_{OPT} \cdot \omega_{px}$. The dimensions of the BTLCD in the X direction are now completely determined and can be obtained using the following expressions: liquid total length in the X direction $L_{Tx} = (2g/\omega_{dx}^2)$; liquid horizontal length in the X direction $L_{hx} = \zeta_x L_{Tx}$; liquid vertical length $L_v = \frac{1}{2}(L_{Tx} - L_{hx})$ and cross sectional area in the X direction (which is equal to the cross section area of the vertical columns because $v_x = 1$): $A_x = m_{fx}/(L_{Tx} \rho_f)$.

For the design in the Y direction, we initially assume that the frequency ratio in the Y direction is equal to the optimum frequency ratio in the X direction, that is, $f_y^0 = f_x|_{OPT}$. The frequency of oscillation and the effective length of the liquid in the Y direction can thus be calculated as follows: $\omega_{dy} = f_y^0 \cdot \omega_{py}$; $L_{ey} = (2g/\omega_{dy}^2)$ (note that in this case, we refer to liquid effective length and not total length because v_y is not necessarily equal to one). We can now calculate the dimensions of the device in the Y direction considering that $L_{ey} = 2L_v + v_y L_{hy}$, and the total liquid mass in the Y is equal to $m_{fy} = \rho_f (2A_v L_v + \frac{A_v}{v_y} L_{hy})$. The solution of this set of simultaneous equations leads to the following:

$$L_{hy} = \sqrt{\left(\frac{L_{ey} - 2L_v}{A_v} \right) \left(\frac{m_{fy}}{\rho_f} - 2A_v L_v \right)} \quad (36)$$

$$v_y = \frac{L_{ey} - 2L_v}{L_{hy}} \quad (37)$$

The shape factor in the Y direction can be calculated as follows: $\zeta_y = \frac{L_{hy}}{L_{Ty}}$, where $L_{Ty} = L_{hy} + 2L_v$, and the value of α_y can be obtained using Equation 6.

All the parameters obtained for the Y direction at this stage of the design process depend on the initial value of the frequency ratio in the Y direction, which was considered to be equal to the optimal

frequency ratio in the X direction. We can now calculate the frequency ratio in the Y direction as a function of the dimensionless parameters, using Equation 19 in the case of negligible damping of the primary structure, or by Equation 22 otherwise, thus finding f_y^1 as $f_y^1 = f|_{OPT}(\mu_y, \alpha_y, \nu_y)$. It should be noted that the value of f_y^1 will not necessarily be equal to f_y^0 , therefore, the design of the BTLCD will involve an iterative process, which will continue until $|f_y^i - f_y^{i-1}| \leq \epsilon$, with ϵ being a tolerance value. This iterative procedure will lead us to the optimum frequency ratio in the Y direction. Due to the fact that the mass ratios in the X and Y directions are often low and similar, this iterative process converges rapidly, as will be demonstrated using an example in the next section.

Before finishing the design, it is important to guarantee that the maximum displacement of the liquid free surface will not surpass the maximum allowable displacement in the vertical columns of the device. If we assume that horizontal cross-sections of the conduits of the device have a rectangular shape, it can be shown that its height shall be equal to $h = \frac{1}{2}\sqrt{2A_y}$; the width of the horizontal conduits parallels to X direction is $w = \frac{1}{2}\nu_y\sqrt{2A_y}$ and the cross sections of the horizontal conduits parallels to Y direction are squares with side equal to h . The maximum allowable displacement in the vertical columns can thus be calculated as $L_{max} = L_v - \frac{1}{2}h$. On the other hand, the maximum displacement of the liquid free surface can be evaluated directly from a time history analysis. As an alternative, the expected deviation of the displacement of the liquid free surface can be estimated from the mean square of the liquid displacement in the X and Y directions, as follows:

$$\sigma_v = \frac{1}{A_v} \left(A_x \sqrt{\mathbb{E}\{u_{dx}^2\}} + A_y \sqrt{\mathbb{E}\{u_{dy}^2\}} \right) \tag{38}$$

We can therefore impose the condition $k \cdot \sigma_v - L_{max} < 0$, where k is a real positive number. If the latter assessment is not true, we must select a lower value of the shape factor in the X direction, in order to increase the value of L_v and thus the allowable space in the vertical columns.

The flow resistance coefficients η_x and η_y can be obtained from Equation 9, in which all the terms shall be evaluated for the optimal design conditions found as described earlier.

7. BIDIRECTIONAL TUNED LIQUID COLUMN DAMPER EXPERIMENTAL ANALYSIS

7.1. Bidirectional tuned liquid column damper and scale model

The BTLCD will be designed to control the response of the first two mode shapes of a 3-story scale model shown in Figure 7. As can be seen in the left side of the figure, the model has a chevron brace system located in each story and connected to the rest of the structure by means of helical springs. This configuration allows to have different periods of oscillation in each direction. The periods of oscillation can be adjusted modifying the number of springs, which in the case under analysis are 20 in each story. The periods of oscillation, damping ratios and mode shapes were identified empirically using the Eigensystem Realization Algorithm (ERA) by means of pullback and hit tests. The results of these tests are shown in the right side of Figure 7.

According to Figure 7, the device will be located in the top story where the largest modal displacement occurs for both controlled modes shapes. The equivalent properties of the single DOF structures can be obtained using the expressions defined in Section 5, that is, effective mass in X direction: $\tilde{m}_1 = \frac{1[kg]}{0.087^2} = 131.5[kg]$, effective stiffness in X direction: $\tilde{k}_1 = \left(1[kg] \cdot (2\pi/1.52[seg])^2 \right) / 0.087^2 = 22.559[Ncm]$, effective mass in Y direction: $\tilde{m}_2 = \frac{1[kg]}{0.085^2} = 138.4[kg]$, effective stiffness in Y direction: $\tilde{k}_2 = \left(1[kg] \cdot (2\pi/1.1[seg])^2 \right) / 0.085^2 = 45.073[Ncm]$. Each step of the design procedure are described next:

1. An initial value of the shape factor, $\zeta_x = 0.7$, and mass ratios $\mu_x = \mu_y = 0.03$ will be considered. Also, the area ratio in X direction is chosen equal to unity. Recalling that $M_{x_{eq}} = \tilde{m}_1$ and $M_{y_{eq}} = \tilde{m}_2$, then from Equation 34 $m_{fx} = 4.62[kg]$ (mass of the conduits and columns of the device has been estimated in 3[kg]).

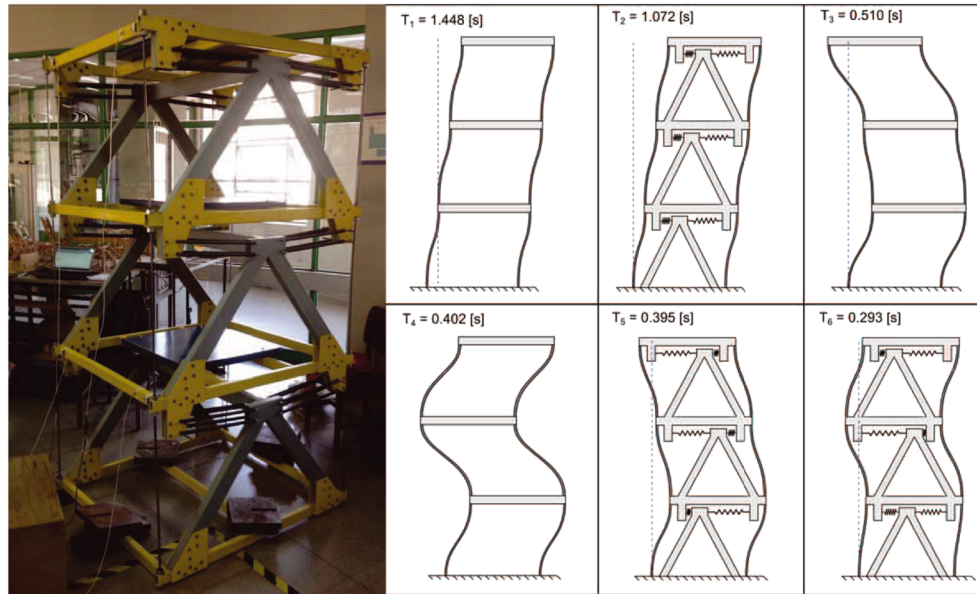


Figure 7. Scale model and its first six translational modes shapes.

2. The total liquid mass in the Y direction can be calculated from Equation 35; $m_{fy} = 4.06[\text{kg}]$. The total liquid mass inside the device can be estimated as follows: $m_f = m_{fy} + \zeta_x m_{fx} = 7.76[\text{kg}]$.
3. Using Equation 19, the value of the optimum frequency ratio is $f_{x|OPT} = 0.976$. The total mass of the first mode equivalent 1 DOF is $M_{Tx} = 131.5[\text{kg}] + 7.76[\text{kg}] + 3[\text{kg}] = 142.26[\text{kg}]$. The value of ω_{px} can be calculated as $\omega_{px} = \sqrt{22.559[\text{Ncm}]/142.26[\text{kg}]} = 3.982[\text{radseg}]$. The device optimum frequency of oscillation in X direction is therefore: $\omega_{dx} = 0.976 \cdot 3.982[\text{radseg}] = 3.886[\text{radseg}]$.
4. The total liquid total length in X direction, which is equal to its effective liquid length because $v_x = 1$, is $L_{Tx} = 2 \cdot 9.81[\text{mse}g^2]/(3.886[\text{radseg}])^2 = 130[\text{cm}]$.
5. The BTLCD dimensions in X direction are as follows: horizontal length $L_{hx} = 0.8 \cdot 130[\text{cm}] = 104[\text{cm}]$; vertical length $L_v = \frac{1}{2}(130[\text{cm}] - 104[\text{cm}]) = 13[\text{cm}]$; cross section area $A_x = 4.62[\text{kg}]/(130[\text{cm}] \cdot 0.001[\text{kgcm}^3]) = 35.54[\text{cm}^2]$.
6. The frequency ratio in Y direction is set equal to the optimum frequency ratio in X direction, thus, $f_y^0 = f_{x|OPT} = 0.976$. The total mass of the second mode equivalent 1 DOF is $M_{Ty} = 138.4[\text{kg}] + 7.76[\text{kg}] + 3[\text{kg}] = 149.16[\text{kg}]$. The value of ω_{py} is $\omega_{py} = \sqrt{45.07[\text{Ncm}]/149.16[\text{kg}]} = 5.497[\text{radseg}]$. Liquid frequency of oscillation in Y direction is $\omega_{dy}^0 = 0.976 \cdot 5.497[\text{radseg}] = 5.364[\text{radseg}]$; and liquid effective length in Y direction is $L_{ey} = 2 \cdot 9.81[\text{mse}g^2]/(5.364[\text{radseg}])^2 = 68.2[\text{cm}]$.
7. The horizontal length in Y can be obtained from Equation 36 where we obtain $L_{hy} = 61[\text{cm}]$; total liquid length in the Y direction: $L_{Ty} = 61[\text{cm}] + 2 \cdot 13[\text{cm}] = 87[\text{cm}]$.
8. Area ratio in the Y direction: $v_y = (68.2[\text{cm}] - 2 \cdot 13[\text{cm}])/61[\text{cm}] = 0.692$; shape factor in the Y direction: $\zeta_y = 61[\text{cm}]/87[\text{cm}] = 0.701$; $\alpha_y = 0.701/(0.692 \cdot (0.692 - 1) + 1) = 0.894$.
9. With the dimensionless parameters of the BTLCD in Y direction, we can calculate the frequency ratio from Equation 27, which lead to $f_y = 0.979$. This value is only 0.33% larger than the assumed frequency ratio in step 6, which reflect the rapid convergence of the design procedure. In this case, one more iteration is performed in order to fulfil with a convergence tolerance of no more of 0.1%. This second iteration leads to the following dimensions of the device in Y direction: total liquid length $L_{Ty} = 86.6[\text{cm}]$; area ratio $v_y = 0.689$; cross section area $A_y = 51.58[\text{cm}^2]$; shape factor $\zeta_y = 0.7$. The cross sections dimensions of the device are $h = 5.1[\text{cm}]$ and $w = 3.5[\text{cm}]$.
10. Finally, the optimal critical damping ratios can be calculated using Equation 24, which leads to following values $\zeta_{dx} = 0.071$ and $\zeta_{dy} = 0.081$.

The result of the design procedure is presented in Figure 8, which shows the device and its overall dimensions. The actual total liquid mass inside the BTLCD reaches 8[kg]. It is important to note that if the BTLCD is replaced by two equivalent and independent TLCs, the total liquid mass would in this case reach 12.67[kg], 58.4% larger than the liquid mass of the proposed BTLCD.

7.2. Experimental parameter estimation of the bidirectional tuned liquid column damper

Experimental shaking table analyses will be performed in order to verify the dynamics properties of the BTLCD. The device is subject to the action of a filtered white noise applied on its base with energy in the 0.4[Hz]–5[Hz] band, and which peak displacement, velocity and acceleration are as follows: 0.054 [m], 0.24[m/seg] and 1.89[m/seg²], respectively. To measure the coupled effects, the BTLCD will be inclined relative to the direction excited by the shaking table, where five inclination angles are investigated, $\theta=0^\circ, 30^\circ, 45^\circ, 60^\circ, 90^\circ$. The periods and critical damping ratios of the BTLCD can be obtained from the transfer functions between the base acceleration and the liquid displacements inside the device. After applying the Fourier transformation to Equation 31, these transfer functions can be expressed as follows:

$$H_d(\omega) = \frac{-\omega v}{\omega_d^2 - \omega^2 + i \cdot 2v\zeta_d \omega_d \omega} \tag{39}$$

where the directional subscripts have been removed for clarity. The transfer functions between the vertical displacements of the free liquid surfaces, and the base acceleration can be obtained using the fact that the total volume of liquid shall be conserved, thus:

$$U_z(\omega) = \pm \frac{1}{v_x} H_x(\omega) \ddot{U}_{sx}(\omega) \pm \frac{1}{v_y} H_y(\omega) \ddot{U}_{sy}(\omega) \tag{40}$$

where $U_z(\omega)$ is the Fourier transform of the vertical liquid free surface, $\ddot{U}_{sx}(\omega)$ and $\ddot{U}_{sy}(\omega)$ are the Fourier transformations of the base accelerations in the X and Y directions, respectively, $H_x(\omega)$ and $H_y(\omega)$ are the transfer functions of the liquid displacements inside the device in X and Y directions, respectively (obtained from Equation 39), and the signs accounts for the directions of the horizontal liquid displacements relative to the vertical column under analysis. Equation 40 can be rewritten in terms of the angle between the base acceleration applied to the device and its principal directions, θ as follows:

$$U_z(\omega) = \left(\pm \frac{\cos(\theta)}{v_x} H_x(\omega) \ddot{U}_{sx}(\omega) \pm \frac{\sin(\theta)}{v_y} H_y(\omega) \ddot{U}_{sy}(\omega) \right) \ddot{U}_s(\omega) = H_z(\omega) \cdot \ddot{U}_s(\omega) \tag{41}$$

where $H_z(\omega)$ is then the transfer function between the vertical displacement of the liquid free surface and the base acceleration. In order to verify the lineal equivalent damping approach described in Section 1, restrictions will be located in the mid sections of the device. The flow resistance coefficients are obtained from Equation 9, using the optimal critical damping ratios found in the previous section and the standard deviation of the liquid velocity estimated using the transfer function between the

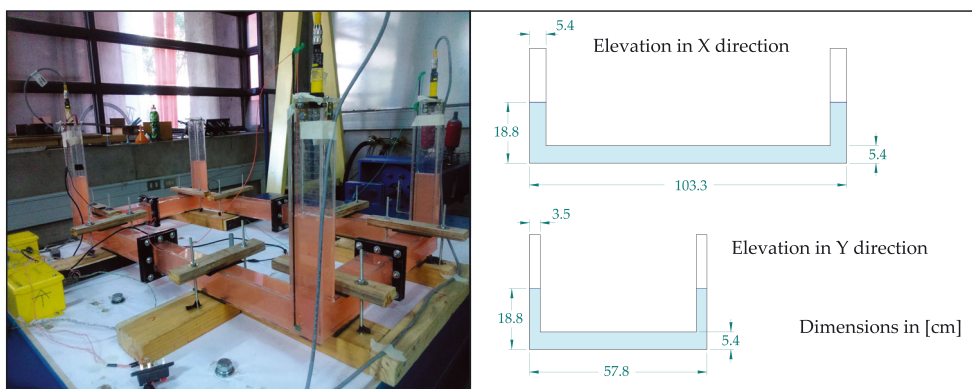


Figure 8. The bidirectional tuned liquid column damper and its main dimensions.

liquid velocity and the base acceleration: $H_v(\omega) = i\omega H_d(\omega)$. The flow resistance coefficients are then $\eta_x = 12.88$ and $\eta_y = 9.16$. The blocking area ratio can now be determined using the results of the study of Wu *et al.* [13], which leads to a blocking ratio equal to 0.59 in X direction and 0.5 in direction Y direction.

In order to validate the damping values obtained from Equation 9, shaking table tests were performed. The BTLCD was subjected to three different filtered white noise processes, in which the duration varies between 10 and 15 min. For each test, empirical damping ratios were identified using the Multivariable Output Error State Space (MOESP) method, and theoretical damping ratios were obtained by Equation 9, where it is consider the standard deviation of the liquid velocity calculated for each one of the time ranges analysed. These results are shown in Figure 9, and it can be seen the good agreement between the mean of the theoretical damping values and the damping values measured experimentally.

As indicated in the beginning of this section, tests were also conducted with different orientations to compare the theoretical transfer function with the experimental one. This results are shown in Figure 10, and the periods of oscillation and the critical damping ratios are summarised in Table I.

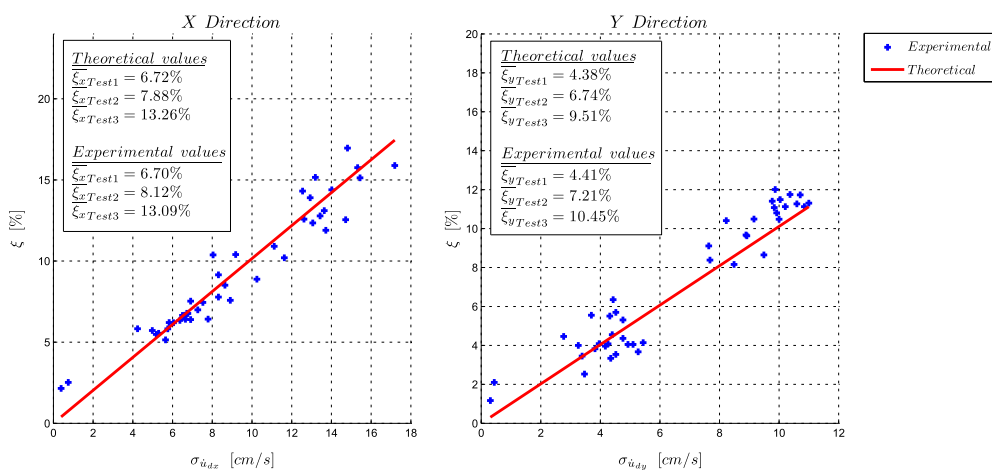


Figure 9. Experimental damping versus damping obtained by Equation 9.

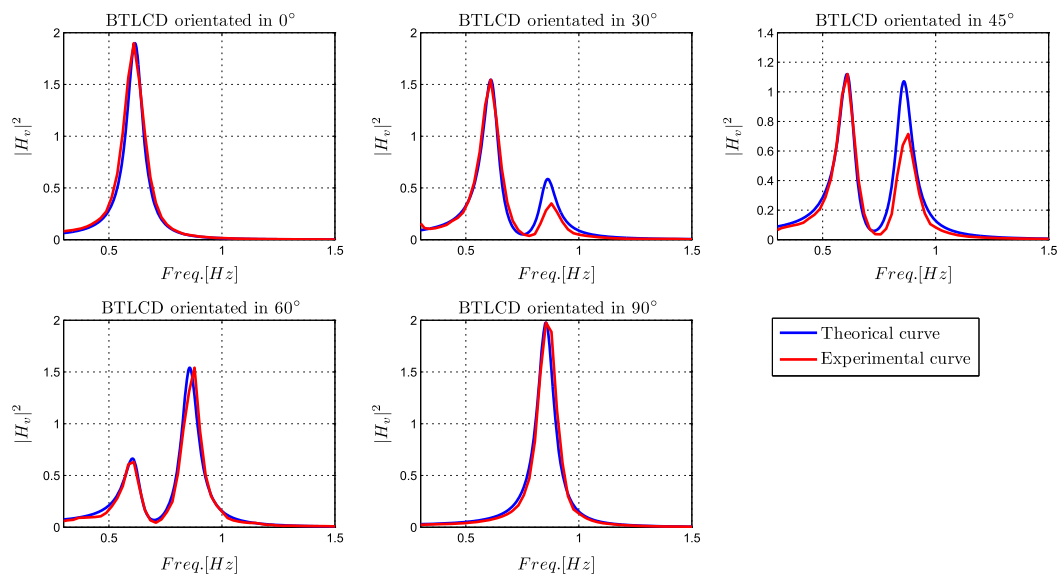


Figure 10. Experimental transfer functions from shaking table acceleration. BTLCD, bidirectional tuned liquid column damper.

Table I. IBidirectional tuned liquid column damper theoretical and measured natural periods and critical damping ratios.

Direction	Theoretical			Measured		
	$f_n[Hz]$	$T_n[seg]$	ζ	$f_n[Hz]$	$T_n[seg]$	ζ
X	0.618	1.618	0.071	0.617	1.622	0.063
Y	0.857	1.167	0.081	0.861	1.161	0.068

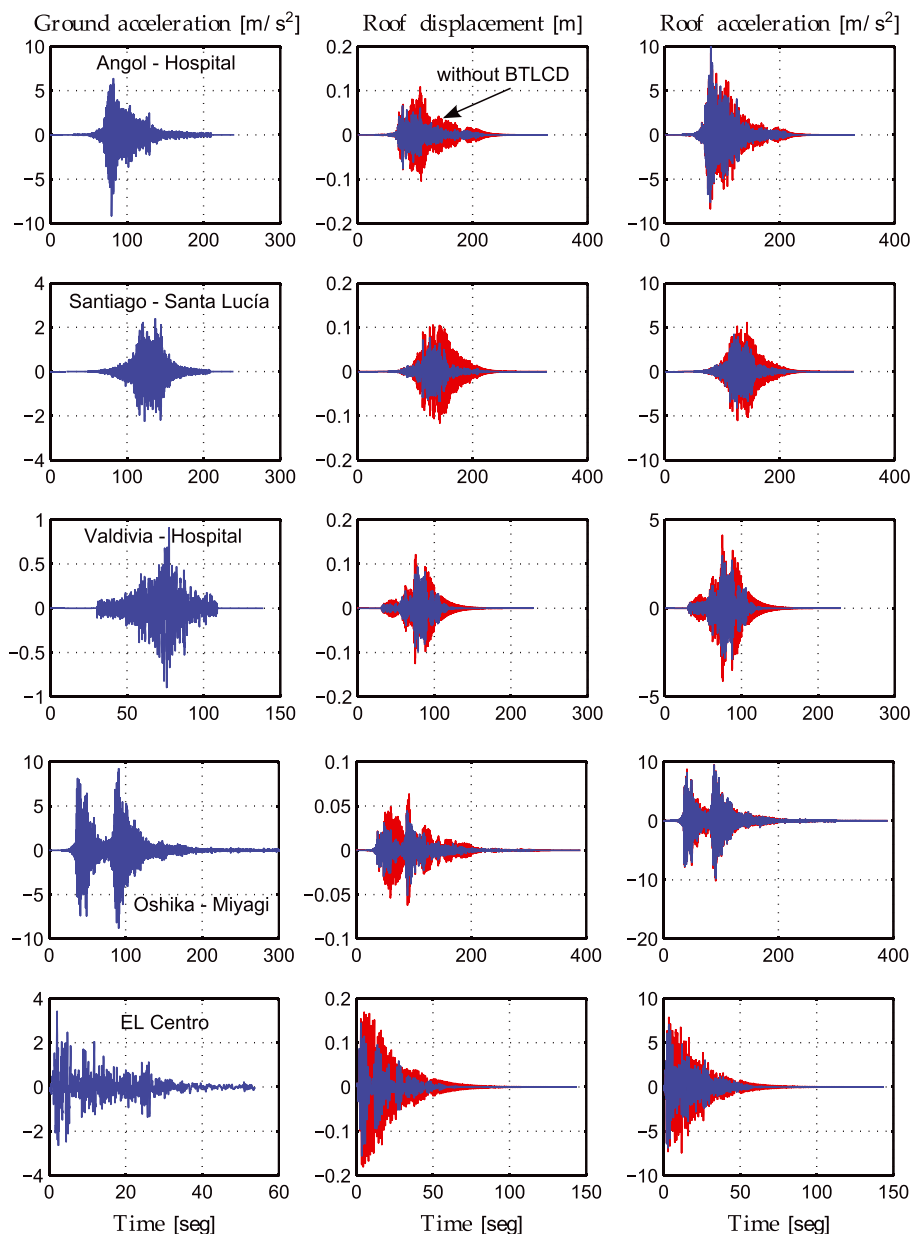


Figure 11. Ground accelerations applied to the system base in the X direction and the corresponding roof displacements and accelerations before and after installing the optimal bidirectional tuned liquid column damper (BTLCD) (red and blue lines, respectively). The ratio of the total liquid mass to the total mass of the primary structure is equal to 0.031(3.1 %).

As is apparent from Table I, the measured dynamic properties of the BTLCD show good agreement with its theoretical dynamic properties. The values of the measured critical damping ratios are slightly lower than its theoretical values, mainly due to the fact that the shaking table filters part of the energy of the filtered white noise. Because of the inherent nonlinear nature of the damping forces, the critical damping ratios are function of the external excitation level. This is clear from Equation 9, in which for a given flow resistance value, the critical damping ratio remains as function of the standard deviation of the liquid velocity. Nevertheless, as shown by Wu *et al.* [13], the performance of the device is not sensitive to the value of the critical damping ratio. The experimentally measured transfer functions are shown in Figure 10, and were obtained averaging in the frequency domain using windows of 30 [seg] with 50% overlap.

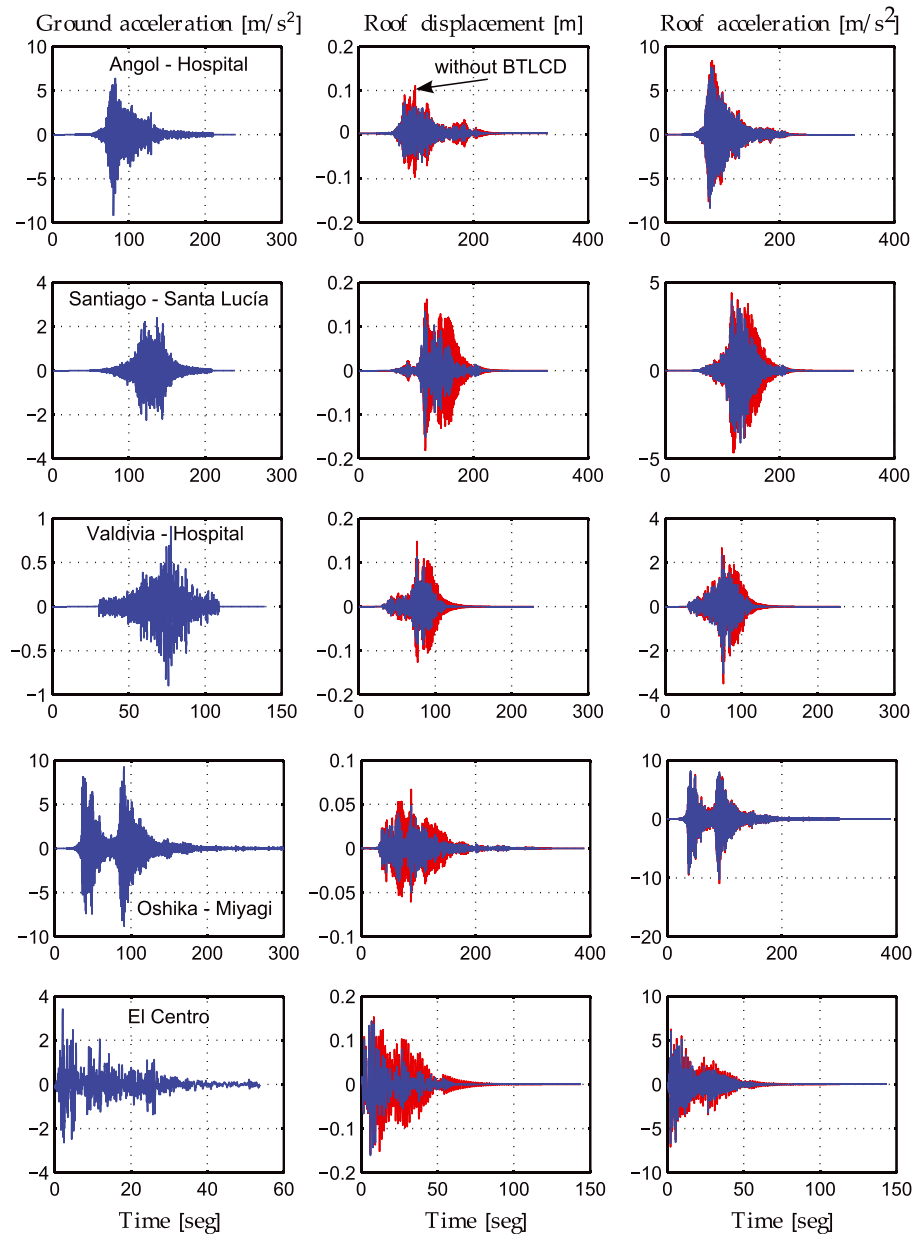


Figure 12. Ground accelerations applied to the system base in the Y direction and the corresponding roof displacements and accelerations before and after installing the optimal tuned liquid column damper (BTLCD) (red and blue lines, respectively). The ratio of the total liquid mass to the total mass of the primary structure is equal to 0.031 (3.1%).

8. SEISMIC NUMERICAL ANALYSIS

To verify the effectiveness of the proposed device, the roof displacement and acceleration time histories of the example structure with and without the proposed BTLCD obtained by numerical analysis of the scale model and the designed BTLCD are shown in Figures 11 and 12. The system is excited using three seismic records, namely, (1) the 2010 Mw = 8.8 Chilean earthquake obtained by the University of Chile and available to the scientific community (<http://terremotos.ing.uchile.cl>); (2) the Oshika-Miyagi seismic record from the 2011 Mw = 9.1 Japanese earthquake obtained from the Japanese seismic network of strong-motion stations (<http://www.k-net.bosai.go.jp/>); and (3) the 1940 El Centro earthquake, Mw = 6.9 record obtained from the COSMOS earthquake web site (<http://db.cosmoseq.org/>). The BTLCD designed according to the optimal parameters and the proposed procedure performs well for the considered earthquake excitations. The reduction of the maximum roof displacement and the rapid response decay are particularly noticeable. Nevertheless, as can be shown from Figures 11 and 12, the reductions in acceleration are negligible. The device in this particular example has been designed to control the responses of the two first vibration modes, which have low spectral accelerations, thus controlling their responses has only a limited influence on the accelerations. Generally speaking, if the purpose is mainly to reduce the acceleration response, then the BTLCD should be designed to control higher modes, with higher spectral accelerations.

9. CONCLUSIONS

In the present study, we have proposed the use of a new device that acts as two independent and orthogonal TLCDs combined in one single BTLCD unit, for the purpose of controlling the seismic response of structures that have vibrations occurring essentially in two mutually perpendicular directions. First, the BTLCD was used as a seismic control device for two DOF structures. Using an equivalent linear formulation of the nonlinear forces from the liquid flow inside the device, by means of Lagrangian dynamics, it was possible to write a set of linear equations of motion of the BTLCD and the two DOF primary structures to be controlled. The optimal tuning parameters of the BTLCD were then obtained by minimising the response of the primary structure when subject to white noise base acceleration. The reductions in the mean square value of the primary structure displacement show that the effectiveness of the BTLCD is greater when it is used to control low damped structures. As the damping of the structure increases, the reductions become smaller; however, in these cases, the use of energy dissipation devices is usually unnecessary. The application of the BTLCD in structures with several degrees of freedom was also studied. In this case, the equations of motion of the BTLCD and the primary structure were written using the vector formulation of Lagrangian dynamics, which leads to a system of equations that can be reduced if the response of the primary structure occurs mainly in two perpendicular modes. Using this consideration, the system of equations was transformed into a system, which is similar to the system of equations for the BTLCD and the two DOF primary structures. The optimal tuning parameter found can then be used to design the BTLCD as a seismic control device for multiple DOF structures. An iterative method of rapid convergence to facilitate the design of the device is proposed. The dynamical properties of the device were determined using experimental analyses, in which the results are in good agreement with the theoretical values. Finally, the example of a 3-story scale model was analysed under the action of five seismic records with and without the BTLCD. The results show that the device performs well, and the reduction of the structure displacement and the rapid response decay obtained revealed that the device increases the damping of the controlled structure.

ACKNOWLEDGEMENTS

The authors would like to thank the K-NET National Research Institute for Earth Science and Disaster Prevention (NIED) and the COSMOS strong motion database for the seismic records used in this study.

REFERENCES

1. Kareem A, Kijewski T, Tamura Y. Mitigation of motions of tall buildings with specific examples of recent applications, 1999.
2. Feng MQ, Mita A. Vibration control of tall buildings using mega sub-configuration. *Journal of Engineering Mechanics* 1995; **121**.
3. Perno S, De Angelis M, Reggio A. Dynamic response and optimal design of structures with large mass ratio TMD. *Earthquake Engineering and Structural Dynamics* 2011; **41**:41–60.

4. Aguirre M, Villaverde R, Hamilton C. Aseismic roof isolation system built with steel oval elements: exploratory study. *Earthquake Spectra* 2005; **21**:225–241.
5. Tsai H-C, Lin G-C. Optimum tuned-mass dampers for minimizing steady-state response of support-excited and damped systems. *Earthquake Engineering & Structural Dynamics* 1993; **22**:957–973.
6. Sadek F, Mohraz B, Taylor AW, Chung RM. A method of estimating the parameters of tuned mass dampers for seismic applications. *Earthquake Engineering & Structural Dynamics* 1997; **26**:617–635.
7. Takewaki I. Soil-structure random response reduction via TMD-VD simultaneous use. *Computer Methods in Applied Mechanics and Engineering* 2000; **190**:677–690.
8. Sakai F, Takaeda S, Tamaki T. Tuned liquid column damper new type device for suppression of building vibrations. Proceedings of International Conference on Highrise Buildings 1989; 926–931.
9. Gao H, Kwok KCS. Optimization of tuned liquid column dampers. *Engineering Structures* 1997; **19**:476–486.
10. Yalla SK, Kareem A. Optimum absorber parameters for tuned liquid column dampers. *Journal of Structural Engineering* 2000; **126**:906–915.
11. Kwok KCS, Hitchcock PA, Shum KM. Closed-form optimum liquid column vibration absorber parameters for base-excited damped structures. *Advances in Structural Engineering* 2011; **14**:489–497.
12. Wu J-S, Hsieh M. Study on the dynamic characteristic of a U-type tuned liquid damper. *Ocean Engineering* 2002; **29**:689–709.
13. Wu J-C, Shih M-H, Lin Y-Y, Shen Y-C. Design guidelines for tuned liquid column damper for structures responding to wind. *Engineering Structures* 2005; **27**:1893–1905.
14. Colwell S, Basu B. Experimental and theoretical investigations of equivalent viscous damping of structures with TLCD for Different fluids. *Journal of Structural Engineering* 2008; **134**:154–163.
15. Ghosh A, Basu B. Seismic vibration control of short period structures using the liquid column damper. *Engineering Structures* 2004; **26**:1905–1913.
16. Ghosh A, Basu B. Seismic vibration control of nonlinear structures using the liquid column damper. *Journal of Structural Engineering* 2008; **134**:146–153.
17. Shum KM, Xu YL, Guo WH. Wind-induced vibration control of long span cable-stayed bridges using multiple pressurized tuned liquid column dampers. *Journal of Wind Engineering and Industrial Aerodynamics* 2008; **96**(2):166–192.
18. Colwell S, Basu B. Tuned liquid column dampers in offshore wind turbines for structural control. *Engineering Structures* 2009; **31**:358–368.
19. Sadek F, Mohraz B, Lew HS. Single and multiple tuned liquid columns dampers for seismic applications. *Earthquake Engineering and Structural Dynamics* 1998; **27**:439–463.
20. Kwok KSC, Samali B, Gao H. Characteristics of multiple tuned liquid column dampers in suppressing structural vibration. *Engineering Structures* 1999; **21**:316–331.
21. Shum KM, Xu YL. Multiple tuned liquid column dampers for reducing coupled lateral and torsional vibration of structures. *Engineering Structures* 2004; **26**:745–758.
22. Hitchcock PA, Kwok KCS, Watkins RD. Characteristics of liquid column vibration absorbers (LCVA) II. *Engineering Structures* 1997; **19**:135–144.
23. Lee S-K, Min K-W, Lee H-R. Parameter identification of New bidirectional tuned liquid column and sloshing dampers. *Journal of Sound and Vibration* 2010; **330**:1312–1327.
24. Tait MJ, Deng X. The performance of structure-tuned liquid damper systems with different tank geometries. *Structural Control and Health Monitoring* 2010; **17**:254–277.
25. Meirovitch L. Analytical Methods in Vibrations. Macmillan Publishing Co: New York, 1967.
26. Blevins RD. Applied Fluid Dynamics Handbook. Van Nostrand Reinhold Company: New York, 1984.
27. Idelchik IE. Handbook of Hydraulic Resistance. Research Institute for Gas Purification: Moscow, Russia, 1986.
28. Roberts JB. Random Vibration and Statistical Linearization. Spanos PD: Dover, 1999.
29. Rüdinger F. Modelling and estimation of damping in non-linear random vibration. PhD thesis, Technical University of Denmark, 2002.
30. Crandall SH, Mark WD. Random Vibration in Mechanical Systems. Academic Press: London, 1963.
31. Rozas L, Boroschek R. Reducción de la Respuesta Estructural por Medio del uso de Disipadores de Masa Sintonizada y Disipadores de Columna Líquida Sintonizada. Master's thesis, Universidad de Chile, 2009.